

# History and Flight Development of the Electrodynamic Dust Shield

Michael R. Johansen\*, Paul J. Mackey†, Michael D. Hogue‡, Rachel E. Cox§, James R. Phillips III ¶  
and Carlos I. Calle ||

*National Aeronautics and Space Administration, Kennedy Space Center, FL, 32899, USA*

The surfaces of the moon, Mars, and that of some asteroids are covered with a layer of dust that may hinder robotic and human exploration missions. During the Apollo missions, for example, lunar dust caused a number of issues including vision obscuration, false instrument readings, contamination, and elevated temperatures. In fact, some equipment neared failure after only 75 hours on the lunar surface due to effects of lunar dust.

NASA's Kennedy Space Center has developed an active technology to remove dust from surfaces during exploration missions. The Electrodynamic Dust Shield (EDS), which consists of a series of embedded electrodes in a high dielectric strength substrate, uses a low power, low frequency signal that produces an electric field wave that travels across the surface. This non-uniform electric field generates dielectrophoretic and electrostatic forces capable of moving dust off of these surfaces. Implementations of the EDS have been developed for solar radiators, optical systems, camera lenses, visors, windows, thermal radiators, and fabrics

The EDS implementation for transparent applications (solar panels, optical systems, windows, etc.) uses transparent indium tin oxide electrodes on glass or transparent film. Extensive testing was performed in a roughly simulated lunar environment (one-sixth gravity at 1 mPa atmospheric pressure) with lunar simulant dust. EDS panels over solar radiators showed dust removal that restored solar panel output reaching values very close to their initial output. EDS implementations for thermal radiator protection (metallic spacecraft surfaces with white thermal paint and reflective films) were also extensively tested at similar high vacuum conditions. Reflectance spectra for these types of implementations showed dust removal efficiencies in the 96% to 99% range. These tests indicate that the EDS technology is now at a Technology Readiness Level of 4 to 5.

As part of EDS development, a flight version is being prepared for several flight opportunities. The flight version of the EDS will incorporate significantly smaller electronics, with an expected mass and volume of 500 g and 350 cm<sup>3</sup> respectively. One of the opportunities is an International Space Station (ISS) experiment : Materials for International Space Station Experiment 10 (MISSE-10). This experiment aims to verify the EDS can withstand the harsh environment of space and will look to closely replicate the solar environment experienced on the moon. A second flight opportunity exists to provide an EDS to several companies as part of NASA's Lunar CATALYST program. The current mission concept would fly the EDS on the footpad of one of the Lunar CATALYST vehicles. Dust will likely deposit on the footpad through normal surface rover activities, but also upon landing where lunar dust is expected to be uplifted. To analyze the effectiveness of the EDS system, photographs of the footpad with one of the spacecrafts onboard cameras are anticipated. If successful in these test flights, the EDS technology will be ready to be used in the protection of actual mission equipment for future NASA and commercial missions to the moon, asteroids, and Mars.

---

\*Research Engineer, Flight Technologies, NASA Kennedy Space Center, and AIAA nonmember

†Physicist, Flight Technologies, NASA Kennedy Space Center, and AIAA nonmember

‡Physicist, Flight Technologies, NASA Kennedy Space Center, and AIAA nonmember

§Mechanical Engineer, Flight Technologies, NASA Kennedy Space Center, and AIAA nonmember

¶Student Intern, Flight Technologies, NASA Kennedy Space Center, and AIAA nonmember

||Senior Research Scientist, Flight Technologies, NASA Kennedy Space Center, and AIAA nonmember

## Nomenclature

$\tau_{MW}$	Maxwell-Wagner charge relaxation time, s
$\epsilon_m$	Dielectric permittivity (medium), $C^2N^{-1}m^{-2}$
$\epsilon_p$	Dielectric permittivity (particle), $C^2N^{-1}m^{-2}$
$\sigma_m$	Electrical conductivity (medium), S/m
$\sigma_p$	Electrical conductivity (particle), S/m
$\omega$	Angular frequency, rad/s
$E$	Electric Field, V/m
$V$	Voltage, V
$L_e$	Characteristic electrode length, m
$k_e$	Electric constant
$q$	charge, C
$t$	time, s
$m$	Mass, kg
$g$	Acceleration due to gravity, $m/s^2$

## I. Introduction

The dusty environments of NASA's future planetary destinations will require careful consideration. Extraterrestrial dust has caused a number of issues in NASA's previous exploration missions. The unweathered lunar dust is extremely jagged from meteoritic bombardment over the millenia. The geometry of the lunar dust and its jagged edges accentuate dust adhesion to surfaces. Figure 1 displays a microscopic image of a lunar dust particle.

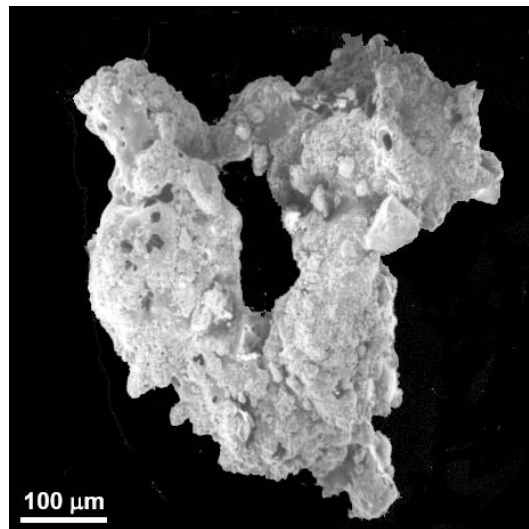


Figure 1: Microscopic imagery of a lunar dust particle. [Credit: NASA]

Along with the jagged nature of the lunar dust, the moon's electrostatic environment is extremely complex and lends itself to dust adhesion. The day side of the lunar surface is charged slightly positive (10 V) due to the photoelectric effect, while the night side of the moon charges negatively on the order of kilovolts as a result of plasma electrons.<sup>1</sup> The cohesive properties of the lunar dust due to the electrostatic charge on the dust particles tend to make the lunar dust adhere to anything it contacts.<sup>2</sup> Figure 2 demonstrates typical dust adhesion experienced during Apollo missions.



Figure 2: Harrison Schmitt during an Apollo 17 EVA covered in fine lunar dust. [Credit: NASA]

Experimental and observational evidence support that fine dust clouds are present on the moon and further lead to the dust deposition and dust adhesion issue for future explorers. Apollo 17 astronaut Gene Cernan noted a “horizon glow” near the lunar terminators that could be attributed to dust particles lofted high above the lunar surface. Recent measurements taken by the Lunar Dust Experiment on the Lunar Atmosphere and Dust Environment Explorer mission show a perpetual lunar dust cloud as a result of high-speed cometary dust particle impacts.<sup>3</sup> In addition, a controversial theory suggests that lunar surface electrostatic potential differences result in electrostatic dust levitation.<sup>4,5</sup>

Mars exploration missions also experience effects as a result of dust accumulation on spacecraft surfaces. Mars is known for local ( $>10^2 \text{ km}^2$ ), regional ( $>10^6 \text{ km}^2$ ), and global dust storms that lift dust particles into the atmosphere and redistribute them across the surface of the planet. The Mars Global Surveyor spacecraft detected 783 dust storms over a 297 day period, with 12 regional dust storms. No global dust storms were noted during this period. The average regional dust storm lasted 10 days and transported  $10^9 \text{ kg}$  of Martian dust.<sup>6</sup> Smaller disturbances, known as dust devils, have been observed with surface and orbital spacecraft. The Mars Exploration Rover, *Spirit*, observed 533 dust devils over a 278 day period and resulted in a calculated atmospheric dust loading of  $19 \text{ kg km}^{-2} \text{ sol}^{-1}$ .<sup>7</sup>

Even during relatively inactive Martian dust storm periods, the Martian atmosphere is still full of micron-sized dust particles that deposit on spacecraft. The Mars Exploration Rovers suffered from reduced power as a result of constant dust deposition from the ever present  $1 \mu\text{m}$  to  $2 \mu\text{m}$  radius dust particles in the Martian atmosphere.<sup>8</sup> The Mars Pathfinder mission, through the Materials Adherence Experiment and Sojourner solar array data, found a dust deposition rate of 0.28% coverage per day on spacecraft surfaces.<sup>9</sup> Stella et al. found that the *Spirit* rover experienced a nearly 20% degradation in solar panel performance over the first 120 sols as a result of dust deposition.<sup>10</sup> Figure 3 displays dust coverage on the solar array of *Spirit*. With current NASA exploration architecture requiring longer stays in these dusty environments than previous missions, a dust mitigation system is necessary.

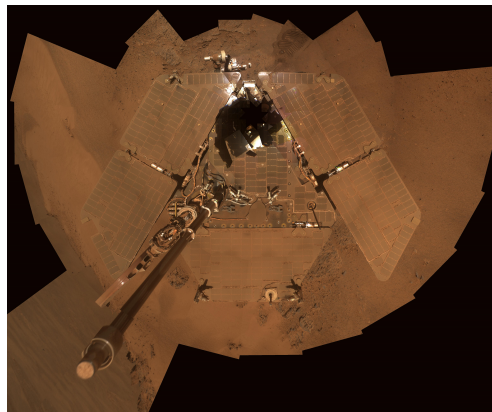


Figure 3: Mars Exploration Rover *Spirit* with fine Martian dust covering its solar array. [Credit: NASA]

## II. Electrodynamic Dust Shield

The Electrodynamic Dust Shield (EDS) employs electrostatic and dielectrophoretic forces to move particles across a surface. The EDS is created by embedding parallel high voltage electrodes into a high dielectric strength substrate in an interdigitated or spiral pattern. It is comprised of a series of conductive and insulative layers, designed to prevent electrical breakdown between the independent electrodes. It removes dust by energizing these independent embedded electrodes with independent high voltage waveforms that are out of phase from one another, thereby generating a traveling electric field wave.<sup>11</sup> Dust particles are observed to hop or slide across the surface as a result, as shown in Figure 4. Sections A and B describe the forces generated by the EDS.

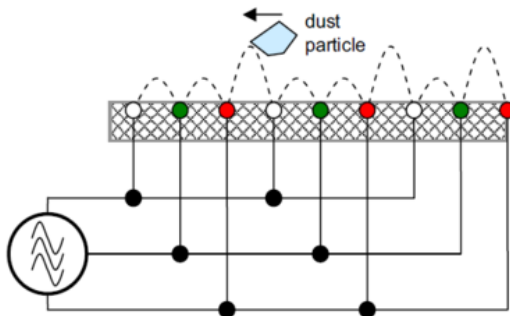


Figure 4: Schematic depicting dust particle motion on a three phase EDS

### A. Dielectrophoretic Force

Dielectrophoresis refers to the force experienced by an uncharged particle in a non-uniform electric field. Its applications span a wide spectrum of scientific and engineering fields, typically used to move or separate particles or cells in a fluid. For a homogeneous sphere with ohmic loss, time averaged dielectrophoresis is shown in Equation 1:

$$\langle \vec{F}_{\text{DEP}} \rangle = 2\pi\epsilon_m R^3 \text{Re}[K(\omega)] \nabla E_{\text{rms}}^2 \quad (1)$$

where  $\epsilon_m$  is the dielectric permittivity of the medium,  $R$  is the particle diameter,  $K$  is the Clausius-Mossotti function,  $\omega$  is the angular frequency, and  $\nabla E$  is the electric field gradient.

The polarizability of a particle, which is dependent on electrical properties of the particle and the medium that surrounds it, plays a crucial role in dielectrophoresis. However, in extreme cases it may only be necessary to take into consideration the dielectric permittivity or the electrical conductivity of both the particle and the medium. To determine what properties are important, the product of the Maxwell-Wagner charge relaxation time and the frequency of the electric field must be considered. According to Jones, the Maxwell-Wagner charge relaxation time characterizes the decay of the dipolar distribution of the free charges on the surface of a sphere. Equation 2 displays the Maxwell-Wagner charge relaxation time, where  $\epsilon$  denotes the dielectric permittivity and  $\sigma$  denotes the electrical conductivity and the subscript m and p denote the medium and particle, respectively.

$$\tau_{\text{MW}} = \frac{\epsilon_p + \epsilon_m}{\sigma_p + 2\sigma_m} \quad (2)$$

Another function that must be considered is the Clausius-Mossotti function. The Clausius-Mossotti function defines whether the particle in question experiences positive dielectrophoresis or negative dielectrophoresis. Positive dielectrophoresis indicates that particles are attracted to electric field intensity maxima and repelled from minima, while in negative dielectrophoresis the opposite effect is noted. Also, the strength of the dielectrophoretic force is dependent on the Clausius-Mossotti function, as shown in Equation 1. Equation 3 displays the frequency dependent form of the Clausius-Mossotti function, as discussed by Benguigui and Lin.<sup>12</sup>

$$\text{Re}[K] = \frac{\epsilon_p - \epsilon_m}{\epsilon_p + 2\epsilon_m} + \frac{3(\epsilon_m\sigma_p - \epsilon_p\sigma_m)}{\tau_{\text{MW}}(\sigma_p + 2\sigma_m)^2(1 + \omega^2\tau_{\text{MW}}^2)} \quad (3)$$

When  $\omega\tau_{MW}$  is much larger than one, only the dielectric permittivity of the particle and medium should be considered for the Clausius-Mossotti function. The angular frequency,  $\omega = 20\pi$  rad/s is used as the high voltage waveform frequency for most EDS applications. With values of  $\sigma_p = 6 \times 10^{-15}$  S m<sup>-113</sup> and  $\epsilon_p = 8.85 \times 10^{-11}$  C<sup>2</sup> N<sup>-1</sup> m<sup>-214</sup> for lunar dust and  $\sigma_m = 0$  (by definition) and  $\epsilon_m = 8.85 \times 10^{-12}$  C<sup>2</sup> N<sup>-1</sup> m<sup>-2</sup> for vacuum, the product,  $\omega\tau_{MW}$ , is sufficiently larger than one, thus the Clausius-Mossotti function becomes

$$\text{Re}[\underline{K}] = \frac{\epsilon_p - \epsilon_m}{\epsilon_p + 2\epsilon_m} \quad (4)$$

An important aspect of the dielectrophoretic force is that it scales with the square of the voltage,  $V$ , and the inverse cube of the characteristic electrode length,  $L_e$ , as shown in Equation 5. As a result, a comparable force can be achieved with a significantly lower voltage by reducing the spacing between two adjacent electrodes.<sup>15</sup>

$$|\overline{F}_{\text{DEP}}| \propto \frac{V^2}{L_e^3} \quad (5)$$

## B. Electrostatic Force

Unlike dielectrophoresis, the electrostatic force requires particle charge. The force is the product of particle charge,  $q$ , and the electric field that the particle experiences,  $E$ . Lunar dust particles are naturally charged due to the complex electrostatic environment.<sup>1</sup> However, they also become tribocharged, or charging due to rubbing, during rover or astronaut activity. In the event of uncharged dust deposited on an EDS, the dust can become charged through particle-particle or particle-EDS collisions as a result of motion caused by the dielectrophoretic force. When the EDS is activated, charged particles are relocated to regions of opposite charge electric field maximas.

A particle also experiences a force based on the charge of the surrounding particles and its own charge. The force is described by Coulomb's law given in Equation 6:

$$\vec{F}_c = k_e q \sum_i \frac{q_i}{r_i^2} \hat{r}_i = q \vec{E} \quad (6)$$

where  $k_e$  is the electric constant,  $q$  is the charge of the particle in question,  $q_i$  is the charge on a particle acting on the particle in question, and  $r_i$  is the distance between the two particles.

For the lunar environment, the viscous forces acting on each particle can be ignored due to the lack of a substantial atmosphere. The net force experienced by a particle when only considering the electrostatic force and force due to gravity was described by Calle et al., shown in Equation 7.<sup>16</sup>

$$m\ddot{r} = qE\cos\omega t - mg \quad (7)$$

Some studies to simulate particle motion caused by the EDS have been conducted. For example, Liu and Marshall modeled particle transport for standing waves<sup>17</sup> and traveling waves.<sup>18</sup> In addition, Malnar et al. completed a 3D simulation of the dielectrophoretic force<sup>19</sup> and Green and Morgan looked specifically at a model for the dielectrophoretic force for interdigitated electrodes.<sup>20</sup> However, due to the complex nature of the forces in play with EDS activation, much of the EDS technology development has been driven by experimental results. The remaining sections describe the EDS development efforts carried out at Kennedy Space Center (KSC).

## C. Types of Dust Shield

KSC has focused its efforts on four variations of the EDS, shown in Figure 5. Each of these systems was developed as the direct result of findings from the Apollo mission reports, where astronauts noted a number of equipment issues caused by lunar dust. The Apollo astronauts noted issues with elevated temperatures on equipment as a result of dust coverage.<sup>21</sup> The copper/Kapton configuration is designed to be coated with thermal paint and attached to spacecraft thermal radiators. The silver/fluorinated ethylene propylene (FEP) shields were also developed for thermal radiators but do not require thermal paint. A carbon nanotube/fabric configuration was developed for space suits, where astronauts noted substantial dust adhesion.<sup>22</sup> Apollo astronauts also noted that visors and other optical equipment were scarred as a result of the abrasive lunar dust.<sup>23</sup> The transparent indium tin oxide (ITO)/glass configuration was developed to protect these systems.

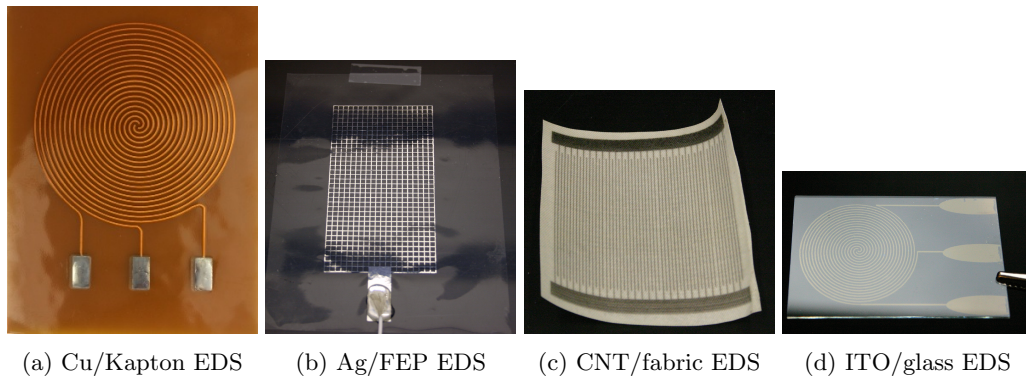


Figure 5: Different substrates and electrode patterns developed for the EDS

KSC has developed one electrode (Figure 5b), two electrode (Figure 5c) and three electrode (Figure 5a) shields. In the one independent electrode (single-phase) configuration, a standing wave is created, as opposed to the traveling wave discussed in Section A. For two independent electrode (2-phase) shields, the high voltage signals sent to the shield are 180 degrees out of phase with one another such that when one electrode is activated the other is not. In the three independent electrode (3-phase) configuration, the three high voltage signals are 120 degrees out of phase from one another.

#### D. Previous Electrostatic Dust Shield Testing

##### 1. Solar Panel Testing

One space application for the EDS is to remove dust from spacecraft solar panels on the surface of the moon, Mars, or asteroids. Calle et al. quantified EDS dust clearing ability on solar panels to show feasibility for this application. The ITO/glass version of the EDS was placed over commercially available 25 cm<sup>2</sup> solar panels to quantify performance. The shields were tested in a vacuum chamber at 1 mPa using 50 μm to 75 μm diameter JSC-1A simulated lunar dust particles. Four ITO electrode configurations were tested in this experiment: with adjacent electrode gaps ranging from 0.48 mm to 0.67 mm. When 20 mg of dust was deposited on each of the dust shields, each solar panel dropped to about 20% of its initial output voltage. Upon EDS activation, each solar panel returned to at least 90% of its original output voltage within two minutes, with all shields returning to at least 98% of their original voltage output after 30 minutes.<sup>16</sup> Figure 6 shows the results from this test.

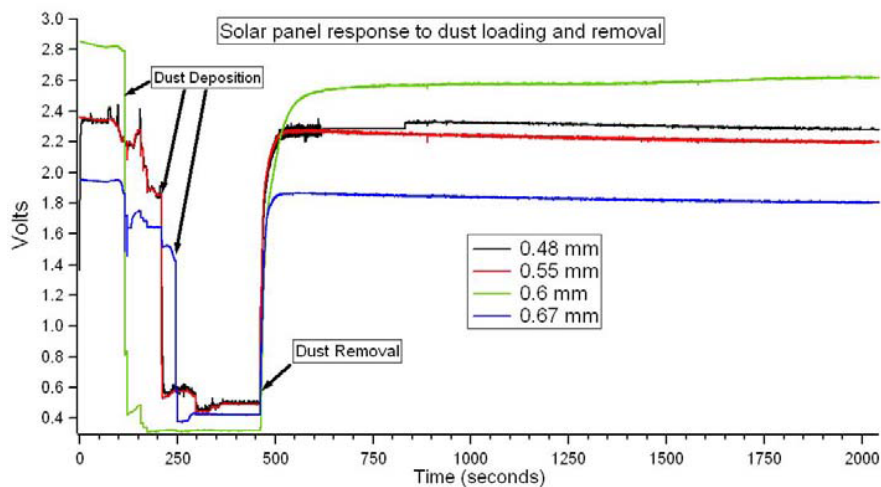


Figure 6: EDS panels with different electrode geometries on solar panels showing clearing efficiencies

## 2. Reflectance Spectra Testing

Another application of the EDS is protecting thermal radiators. Thermal radiators are designed to regulate temperatures on spacecraft by rejecting heat into space. When the radiators become dirty as a result of dust deposition, they are not able to effectively reject heat. Two types of dust shield were created to protect thermal radiators from dust. The copper/Kapton configuration is painted with a white thermal paint to reflect sunlight from spacecraft, while the reflective properties of the silver/FEP or aluminum/FEP shield reflects sunlight without the need for a thermal paint. To test the effectiveness of these two types of EDS, Calle et al. tested the reflective properties of the dust shield in the following configurations: copper/Kapton painted with AZ-93 thermal paint, silver/FEP and aluminum/FEP. In a vacuum chamber at 1 mPa, 50 mg of dust was deposited on each of the previously described dust shields. A UV-Visible-Near Infrared spectrophotometer was used to gather reflectance data with pristine EDS samples and after the deposited dust was removed. All shields returned to 96-99% of their initial reflectance after dust shield activation, shown in Figure 7.

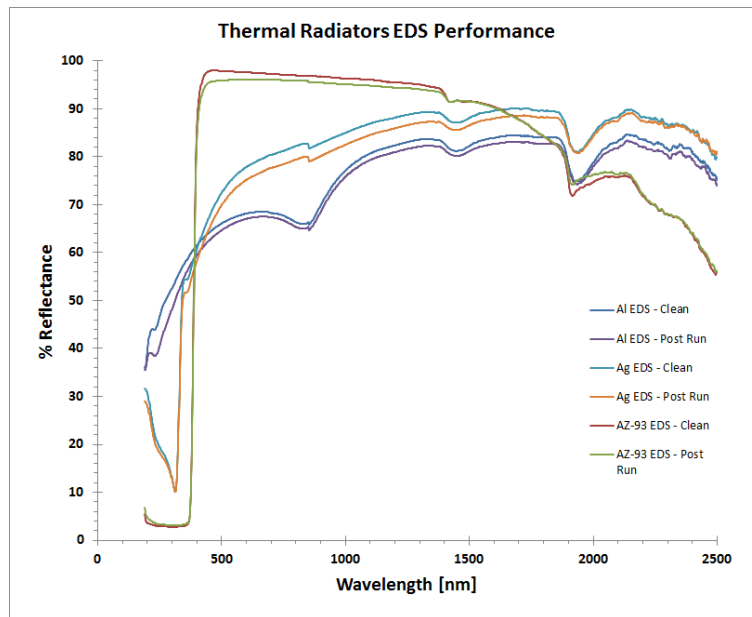


Figure 7: Reflectance spectra of various EDS configurations

## 3. Desert RATS

To demonstrate the scalability of the Electrodynamic Dust Shield, large panels were fabricated and tested on the Habitat Demonstration Unit (HDU) at the annual Desert Research and Technology Study (Desert RATS) event. Two types of large scale EDS were created for this test: a 20 cm diameter transparent and flexible circular EDS made with ITO and polyethylene terephthalate film and a 20 cm  $\times$  20 cm copper and Kapton configuration. In each case, the electrodes were laid out in a 2-phase design. Two of the copper/kapton shields were painted with A-276 thermal paint and two were left unpainted. One painted and one unpainted copper/Kapton shield were coated with a super-hydrophobic Lotus coating developed by Goddard Space Flight Center.<sup>24</sup> The transparent EDS was placed over the Pressurized Excursion Module viewport.<sup>25</sup>

## 4. Reduced Gravity Flights

In order to verify dust shield performance in a simulated lunar environment, KSC researchers, with support from Langley Research Center, flew the ITO/glass EDS configuration on two reduced gravity flights. The objective of the testing was to closely simulate the lunar environment. The tests were conducted in a vacuum chamber (evacuated to 1 mPa) on the NASA C-9 aircraft and also the Zero G Corporation Boeing 727-200. JSC-1A lunar regolith simulant and actual lunar dust samples from Apollo 16 were used during the tests. The dust shield adequately cleared dust up to 450  $\mu$ m in diameter under simulated lunar gravity and pressure.<sup>26</sup>

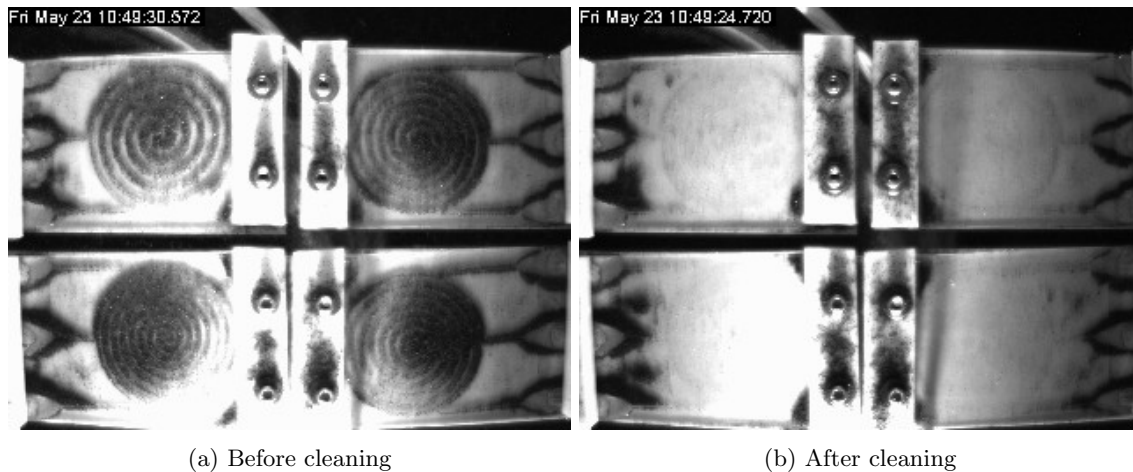


Figure 8: Before and after operation of the glass EDS in a simulated lunar environment

### III. Flight Opportunities

#### A. MISSE

The harsh thermal and radiation environment of space can cause degradation or failure. For example, during Hubble Servicing Mission 2 astronauts noted severe degradation of the multilayer insulation on the Hubble Space Telescope due to electron, proton, ultraviolet, and x-ray radiation as well as effects of thermal cycling.<sup>27</sup> A number of payloads have been developed to better understand how materials and systems respond in the space environment. The results from these tests, such as the Materials International Space Station Experiment (MISSE), are used to further understand how materials respond and to develop materials and systems for future space exploration. MISSE is designed to attach to the exterior of the ISS and is used to test the effects of atomic oxygen, ultraviolet rays, radiation, vacuum, thermal cycling, and micrometeoroids on current and future materials used in space exploration.<sup>28</sup> MISSE offers a number of payload orientations to accommodate individual experiment needs. For example, to simulate the radiation environment on the moon, an experiment can be placed in the aft-facing, or wake, position.

In early 2017, the EDS will fly on MISSE-10 to verify that the multilayer shield design can survive and operate in space. The radiation environment in the wake orientation, where the EDS experiment will be located on the MISSE-10 payload, will roughly simulate what can be expected on the lunar surface. The current mission concept is to activate a copper/Kapton and ITO/glass shield with high voltage pulses and acquire data from the power supply on overall system performance. A large spike in current while the EDS is operating will indicate material breakdown. In addition, photos of the EDS panels will allow researchers to obtain a visual representation of panel health.

#### B. Lunar CATALYST

NASA's Lunar Cargo and Transportation and Landing by Soft Touchdown (Lunar CATALYST) initiative provides a means for NASA to provide technical expertise, test facilities and loan equipment or software for spacecraft development and testing on a no funds exchanged basis. Three U.S. companies were selected for partnership agreements with the agency: Astrobotic Technology, Inc., Masten Space Systems, Inc., and Moon Express, Inc. The intent of the partnerships is to advance commercial lunar lander capabilities and science and exploration missions of interest to NASA and academia.

In anticipation of the CATALYST partners having an interest in the EDS technology, NASA is developing a system capable of operating on the surface of the moon. Smaller electronics, 500 g and 350 cm<sup>3</sup> are currently being developed to survive the harsh lunar environment. Of particular concern is the lunar surface temperature. Lunar surface equatorial temperatures reach 400 K, while nighttime temperatures have been known to drop below 100 K. In fact, some permanently shadowed regions of the lunar surface have a maximum surface temperature of just 30 K.<sup>29</sup>

One challenge in the Lunar CATALYST EDS development is a lack of environmental and operational requirements, since the unit is being developed proactively with the anticipation of one of the CATALYST partners requesting the technology during their development effort. Of particular concern is the survivability of the EDS with the elevated temperatures experienced on the lunar surface. It is impractical to develop a system to operate throughout the full range of temperatures at different locations on the moon. However, designing a system to survive at a given lunar location is possible. In March 2014, the NASA CATALYST partner Astrobotic Technologies, Inc. announced that its first landing location would be at *Lacus Mortis*, a region of the moon at roughly 45 degrees N lunar latitude. The NASA EDS development team is currently using this destination in the payloads preliminary design.

The current mission concept is to place the EDS shields and all supporting electronics on the footpad of a CATALYST partner lunar lander. It is expected that lunar dust will accumulate on the EDS through exhaust plume effects when the spacecraft is preparing to land on the lunar surface and also through operational activities by the lander or rover on the surface of the moon. To verify that the dust shield successfully operates, it is anticipated that photos of the EDS before and after dust clearing will be taken by the spacecraft.

## References

- <sup>1</sup>C. Calle, "The electrostatic environments of mars and the moon," in *Journal of Physics: Conference Series*, vol. 301, no. 1. IOP Publishing, 2011, p. 012006.
- <sup>2</sup>J. A. McDivitt *et al.*, "Apollo 12 mission report," *MSC-01855, March, 1970*.
- <sup>3</sup>M. Horányi, J. Szalay, S. Kempf, J. Schmidt, E. Grün, R. Srama, and Z. Sternovsky, "A permanent, asymmetric dust cloud around the moon," *Nature*, vol. 522, no. 7556, pp. 324–326, 2015.
- <sup>4</sup>T. Gold and G. Williams, "Electrostatic transportation of dust on the moon," in *Photon and Particle Interactions with Surfaces in Space*. Springer, 1973, pp. 557–560.
- <sup>5</sup>J. E. Colwell, S. R. Robertson, M. Horányi, X. Wang, A. Poppe, and P. Wheeler, "Lunar dust levitation," *Journal of Aerospace Engineering*, 2009.
- <sup>6</sup>B. A. Cantor, P. B. James, M. Caplinger, and M. J. Wolff, "Martian dust storms: 1999 mars orbiter camera observations," *Journal of Geophysical Research: Planets (1991–2012)*, vol. 106, no. E10, pp. 23 653–23 687, 2001.
- <sup>7</sup>R. Greeley, P. L. Whelley, R. E. Arvidson, N. A. Cabrol, D. J. Foley, B. J. Franklin, P. G. Geissler, M. P. Golombek, R. O. Kuzmin, G. A. Landis *et al.*, "Active dust devils in gusev crater, mars: observations from the mars exploration rover spirit," *Journal of Geophysical Research: Planets (1991–2012)*, vol. 111, no. E12, 2006.
- <sup>8</sup>G. Landis, K. Herkenhoff, R. Greeley, S. Thompson, P. Whelley *et al.*, "Dust and sand deposition on the mer solar arrays as viewed by the microscopic imager," in *37th Annual Lunar and Planetary Science Conference*, vol. 37, 2006, p. 1932.
- <sup>9</sup>G. A. Landis and P. P. Jenkins, "Measurement of the settling rate of atmospheric dust on mars by the mae instrument on mars pathfinder," *Journal of Geophysical Research: Planets (1991–2012)*, vol. 105, no. E1, pp. 1855–1857, 2000.
- <sup>10</sup>P. M. Stella, R. C. Ewell, and J. J. Hoskin, "Design and performance of the mer (mars exploration rovers) solar arrays," in *Photovoltaic Specialists Conference, 2005. Conference Record of the Thirty-first IEEE*. IEEE, 2005, pp. 626–630.
- <sup>11</sup>C. Calle, C. Buhler, M. Johansen, M. Hogue, and S. Snyder, "Active dust control and mitigation technology for lunar and martian exploration," *Acta Astronautica*, vol. 69, no. 11, pp. 1082–1088, 2011.
- <sup>12</sup>L. Benguigui and I. Lin, "More about the dielectrophoretic force," *Journal of Applied Physics*, vol. 53, no. 2, pp. 1141–1143, 1982.
- <sup>13</sup>G. Olhoeft, D. Strangway, and A. Frisillo, "Lunar sample electrical properties," in *Lunar and Planetary Science Conference Proceedings*, vol. 4, 1973, p. 3133.
- <sup>14</sup>D. Strangway, G. Pearce, and G. Olhoeft, "Magnetic and dielectric properties of lunar samples," *NASA Special Publication*, vol. 370, pp. 417–431, 1977.
- <sup>15</sup>A. Bahaj and A. Bailey, "Dielectrophoresis of microscopic particles," 1979.
- <sup>16</sup>C. Calle, C. Buhler, J. McFall, and S. Snyder, "Particle removal by electrostatic and dielectrophoretic forces for dust control during lunar exploration missions," *Journal of Electrostatics*, vol. 67, no. 2, pp. 89–92, 2009.
- <sup>17</sup>G. Liu and J. Marshall, "Particle transport by standing waves on an electric curtain," *Journal of Electrostatics*, vol. 68, no. 4, pp. 289–298, 2010.
- <sup>18</sup>—, "Effect of particle adhesion and interactions on motion by traveling waves on an electric curtain," *Journal of Electrostatics*, vol. 68, no. 2, pp. 179–189, 2010.
- <sup>19</sup>B. Malnar, W. Balachandran, and F. Cecelja, "3d simulation of traveling wave dielectrophoretic force on particles."
- <sup>20</sup>N. G. Green, A. Ramos, and H. Morgan, "Numerical solution of the dielectrophoretic and travelling wave forces for interdigitated electrode arrays using the finite element method," *Journal of Electrostatics*, vol. 56, no. 2, pp. 235–254, 2002.
- <sup>21</sup>O. G. Morris *et al.*, "Apollo 16 mission report," 1972.
- <sup>22</sup>P. O. L. MODULE and M. S. CENTER, "Apollo 11 mission report," 1971.
- <sup>23</sup>O. G. Morris *et al.*, "Apollo 17 mission report," 1973.
- <sup>24</sup>D. V. Margiotta, K. R. McKittrick, M. Rodriguez, W. C. Peters, S. A. Straka, and C. B. Jones, "Desert research and technology studies exposure of lotus coated electrodynamic shield samples," in *3rd AIAA Atmospheric Space Environments Conference*, 2011, p. 3677.

<sup>25</sup>C. Calle, A. Chen, C. Immer, M. Csonka, M. Hogue, S. Snyder, M. Rogriquez, and D. Margiotta, “Dust removal technology demonstration for a lunar habitat,” in *AIAA Space 2010 Conf. and Exposition, American Institute of Aeronautics and Astronautics (AIAA), Reston, VA*, 2010.

<sup>26</sup>C. Calle, E. Arens, J. McFall, C. Buhler, S. Snyder, J. Geiger, R. Hafley, K. Taminger, and C. Mercer, “Reduced gravity flight demonstration of the dust shield technology for optical systems,” in *Aerospace conference, 2009 IEEE*. IEEE, 2009, pp. 1–10.

<sup>27</sup>J. A. Townsend, P. A. Hansen, J. A. Dever, K. K. de Groh, B. A. Banks, L. Wang, and C. He, “Hubble space telescope metallized teflon® fep thermal control materials: on-orbit degradation and post-retrieval analysis,” *High Performance Polymers*, vol. 11, no. 1, pp. 81–99, 1999.

<sup>28</sup>J. A. Robinson, T. L. Thumm, and D. A. Thomas, “Nasa utilization of the international space station and the vision for space exploration,” *Acta Astronautica*, vol. 61, no. 1, pp. 176–184, 2007.

<sup>29</sup>A. R. Vasavada, J. L. Bandfield, B. T. Greenhagen, P. O. Hayne, M. A. Siegler, J.-P. Williams, and D. A. Paige, “Lunar equatorial surface temperatures and regolith properties from the diviner lunar radiometer experiment,” *Journal of Geophysical Research: Planets (1991–2012)*, vol. 117, no. E12, 2012.